NJC

Accepted Manuscript

This is an *Accepted Manuscript*, which has been through the Royal Society of Chemistry peer review process and has been accepted for publication.

Accepted Manuscripts are published online shortly after acceptance, before technical editing, formatting and proof reading. Using this free service, authors can make their results available to the community, in citable form, before we publish the edited article. We will replace this *Accepted Manuscript* with the edited and formatted *Advance Article* as soon as it is available.

You can find more information about *Accepted Manuscripts* in the Information for Authors.

Please note that technical editing may introduce minor changes to the text and/or graphics, which may alter content. The journal's standard Terms & Conditions and the Ethical guidelines still apply. In no event shall the Royal Society of Chemistry be held responsible for any errors or omissions in this *Accepted Manuscript* or any consequences arising from the use of any information it contains.

ROYAL SOCIETY OF CHEMISTRY

www.rsc.org/njc

New Journal of Chemistry

ARTICLE

RAPTA-C incorporation and controlled delivery from MIL-100(Fe) nanoparticles

Received 00th January 20xx,
Accepted 00th January 20xx

DOI: 10.1039/x0xx00000x

www.rsc.org/

Sara Rojas, Francisco J. Carmona, Carmen R. Maldonado, Elisa Barea and Jorge A. R. Navarro*

$[Fe_3F(H_2O)_2O(btc)_2]\cdot nH_2O$ (H_3btc: benzene-1,3,5-tricarboxylic acid) (MIL-100(Fe)) in the form of nanoparticles with average size of 135 ± 70 nm can be used for the adsorption and controlled delivery of metallodrug [Ru(*p*-cymene)Cl_2(pta)] (RAPTA-C) in simulated body fluid (SBF). The results show that the RAPTA-C delivery process takes place in two steps exhibiting half-lifes of 1.9 and 30 h. We have also found a positive effect of serum bovine albumin (SBA) in promoting the colloidal stability of MIL-100(Fe)@RAPTA-C nanoparticles in SBF as well as in speeding up RAPTA-C delivery rate, which agrees with the suitability of MIL-100(Fe) as drug delivery system (DDS) for the controlled release of RAPTA-C.

Introduction

Cancer is one of the most important causes of death worldwide. Only in Europe, a total of 1.3 millions of cancer deaths are predicted accounting for the estimates of cancer mortality statistics in the present year.[1] Despite the rising incidence of cancer, life expectancy of patients is increasing in recent years. Nowadays, about 50-70% of the cancer patients are treated with drugs based on *cisplatin* and related platinum compounds.[2] However, the lack of specificity of the interaction of *cisplatin* with the desired biological target (DNA), results in a low selectivity of treatment, which involves numerous adverse side effects (nausea, vomiting, nephrotoxicity, etc.) and the development of resistance. These limitations have prompted the search of other antitumor agents based on more effective and less toxic metals. Noteworthy, Ru is receiving a considerable attention as a result of its low toxicity, due to its ability to mimic iron, and the preferred entry into cancer cells versus healthy cell.[3] Moreover, Ru-compounds are capable to interact with multiple extracellular and intracellular targets which make difficult the development of cellular mechanisms of resistance.[4]

In the last 30 years, a variety of Ru-compounds with anticancer activity have been developed, namely, the Ru(III) compounds KP1019, (IndH)*trans*-[$RuCl_4(Ind)_2$] (Ind: indazole) exhibiting activity towards *cisplatin*-resistant native colorectal tumour[5] and NAMI-A (ImH)*trans*-[$RuCl_4$(Im)(DMSO-S)] (Im: imidazole) inhibiting the development and growth of pulmonary metastasic cancer cells.[6] More recently, Ru(II) organometallic compounds, such as [Ru(*p*-cymene)Cl_2(pta)] (pta: 1,3,5-triaza-7-phosphanoadamantane), named RAPTA-C (Figure 1) showing some advantageous features, including amphiphilic nature,[7] interaction with different targets (DNA, proteins).[8] Noteworthy, although this system exhibits low cytotoxicity *in vitro* ($IC_{50\ RAPTA\text{-}C}$ = 507 µM in TS/A murine adenocarcinoma cell line),[9] it does exhibits *in vivo* antitumor activity,[10] and inhibition of metastasis and angiogenesis.[11] Moreover, pta is a very stable phospine possessing advantageous features related to its protonation state which influences its solubility properties and cell membrane permeability.[12] Noteworthy, the pKa value for pta protonation is within the physiological range, with the lower pH values inside the cancer cells favoring its trapping in its protonated form.[7,13] This behavior explains why RAPTA-C is selective against tumor cells and has few side effects. Taking all the above, it would be highly beneficial for patients to find methods for the controlled delivery of this novel metallodrug.

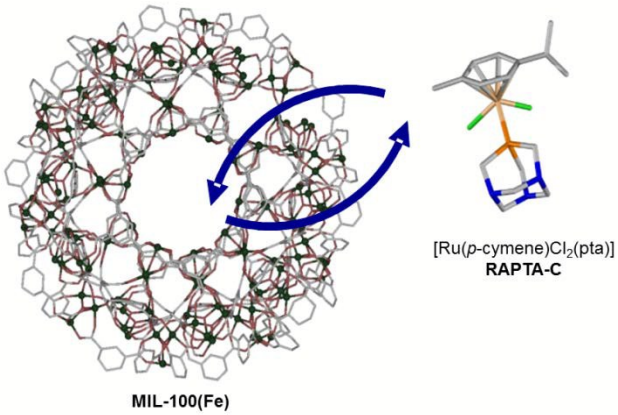

Figure 1. Schematic representation of incorporation and release of anti-tumor metallodrug [Ru(*p*-cymene)Cl_2(pta)] (RAPTA-C) on $[Fe_3F(H_2O)_2O(btc)_2]$ (MIL-100(Fe)).

Departamento de Química Inorgánica, Universidad de Granada, Av. Fuentenueva S/N, 18071, Granada, Spain. E-mail: jarn@ugr.es; Tel: +34 958 248 093
† Footnotes relating to the title and/or authors should appear here.
Electronic Supplementary Information (ESI) available: Experimental details of the methodology employed can be found in ESI. See DOI: 10.1039/x0xx00000x

In this regard, Metal Organic Frameworks (MOFs) are receiving attention as suitable controlled drug-delivery systems (DDS). In this line, we have previously shown the suitability of a robust Ni(II) bipyrazolate MOF for the incorporation and release of RAPTA-C, as a proof-of-concept study.[14] However, Ni(II) toxicity is a major concern and, consequently, the use of MOF systems based on nontoxic metal ions should be desirable. Indeed, $[Fe_3F(H_2O)_2O(btc)_2]\cdot nH_2O$ (H_3btc: benzene-1,3,5-tricarboxylic acid), known as MIL-100(Fe) possess a variety of interesting features related to its composition and structure, that make it an adequate candidate to be used as DDS nanocarrier:[15,16] *i)* MIL-100(Fe) is highly porous (BET surface area of 1700 $m^2\ g^{-1}$) and shows mesoporous voids of 2.5 and 2.9 nm;[17] *ii)* this MOF is built up from Fe(III) biocompatible metal ions;[18] *iii)* it can be prepared as homogeneous and stable nanoparticles with an optimal colloidal stability in different physiological media[19] and *iv)* it is a non-toxic and biodegradable material.[20] Taking into account these characteristics, we are reporting here the possible suitability of MIL-100(Fe) in the adsorption and controlled delivery of RAPTA-C (Figure 1).

Results and Discussion

MIL-100(Fe): synthesis and characterization

The porous material MIL-100(Fe) was synthesized according to the literature methods.[21] In a typical synthesis, we used a mixture based on metallic iron, H_3btc and HF, in HNO_3 and H_2O. This mixture was reacted under hydrothermal conditions at 160 °C during 8 hours giving rise to the formation of MIL-100(Fe) as a microcrystalline orange solid. The as synthesized MIL-100(Fe) was further purified by a two-step process using double solvent extraction with hot water and ethanol in order to eliminate any residual free H_3btc ligand (see Supporting Information for further details). The XRPD, Elemental Analysis (EA) and N_2 adsorption at 77 K of the solid material confirmed phase purity of MIL-100(Fe), whereas transmission electron microscopy (HR-TEM) indicated the formation of nanoparticles, with average size of 135 ± 70 nm, which is in line with previously reported results.[18]

RAPTA-C incorporation

After the assessment of the phase purity and porosity of the prepared MIL-100(Fe), we proceeded to evaluate the suitability of this system for the encapsulation and the controlled delivery of RAPTA-C. With this focus in mind, we proceeded with the incorporation of RAPTA-C into the porous matrix MIL-100(Fe) by means of suspending MIL-100(Fe) (100 mg; 56 µmol) in an absolute ethanol solution of RAPTA-C (86 mM, 10 mL), at room temperature under stirring. UV-vis spectra of aliquots of the supernatant solution proved that the adsorption equilibrium was reached after 4 hours. Finally, the suspension was filtered and washed with absolute ethanol giving rise to loaded matrix MIL-100(Fe)@RAPTA-C. UV-vis, EA and attenuated total reflectance infrared spectroscopy (ATR) studies showed that a significant amount of RAPTA-C is incorporated into the porous matrix of MIL-100(Fe), namely 0.8 mmol of RAPTA-C *per* mmol of MIL-100(Fe) (0.42 g of RAPTA-C *per* g of MIL-100(Fe)) by using this impregnation method. This amount accounts for approx. 14 RAPTA-C molecules per large cage and 7 RAPTA-C per small cage of MIL-100(Fe), considering the RAPTA-C molecules of 0.9 nm[22] occupying both cages with the same pore volume filling ratio. In addition, HR-TEM images demonstrated that the size of the nanoparticles is maintained after the loading of the drug.

The actual incorporation of RAPTA-C into the MIL-100(Fe) cavities was further demonstrated by: *i)* the dramatic reduction of the N_2 adsorption capacity of the MOF at 77 K, indeed BET surface drops from 1657 $m^2\ g^{-1}$ for the pristine material to 497 $m^2\ g^{-1}$ after the RAPTA-C loading (Figure 2); *ii)* the presence of some characteristic peaks of the pure metallodrug in the IR spectrum of MIL-100(Fe)@RAPTA-C (see ESI); *iii)* the increase of the thermal stability of MIL-100(Fe)@RAPTA-C material compared with the original material MIL-100(Fe) (see ESI); *iv*) the XRPD studies after metallodrug incorporation which are indicative that the MOF material maintains its structural integrity after the incorporation of RAPTA-C (see ESI); and *v*) the energy-dispersive X-ray spectroscopy (EDX) analysis confirms the presence of ruthenium and phosphorous in MIL-100(Fe)@RAPTA-C nanoparticles.

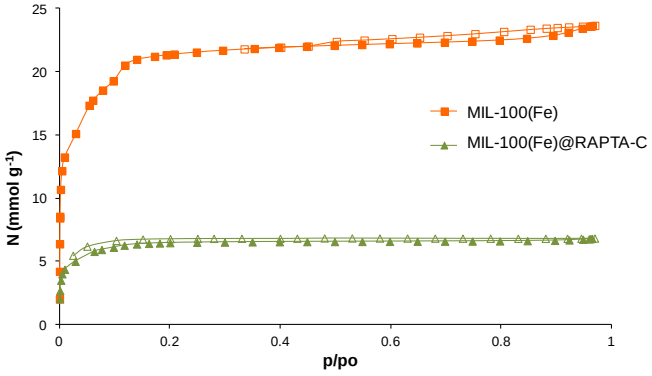

Figure 2. N_2 (77 K) adsorption isotherms for activated MIL-100(Fe) (orange squares) and the RAPTA-C loaded MIL-100(Fe)@RAPTA-C product (green triangles). Empty symbols indicate desorption.

The actual saturation of MIL-100(Fe) porous structure with RAPTA-C metallodrug, in spite of the remaining porosity found in MIL-100(Fe)@RAPTA-C, can be concluded by the fact that different experiments performed in order to increase the amount of adsorbed RAPTA-C into the porous structure of MIL-100(Fe) have not led to any increase on the metallodrug loading capacity.

RAPTA-C delivery

Once the porous matrix of MIL-100(Fe) was loaded with the Ru-metallodrug, we evaluated the ability of the loaded MIL-100(Fe)@RAPTA-C material to deliver RAPTA-C in order to consider the possible use of this system as drug delivery

system (DDS). Bearing in mind the composition of human serum, we studied the RAPTA-C delivery in two different media at 37 ºC for 6 days: *i)* simulated body fluid (SBF), and *ii)* SBF supplemented with bovine serum albumin (SBF@BSA, 5.4% w/v). In this regard, it should be noted that albumin is the most abundant protein in mammals' blood plasma and has been shown to slowdown the degradation rate of the MIL-100(Fe) nanoparticles during 24 hours, as well as, to improve their colloidal stability.[19]

We studied the RAPTA-C delivery kinetics by determining the amount of desorbed RAPTA-C in the supernatant solution of SBF at 37 °C at different intervals of time by means of UV-vis and RP-HPLC. The UV-vis results obtained using a constant volume of SBF (100 mL) showed that the RAPTA-C delivery occurs in two stages (Figure 3). A possible explanation of this two stage process might be related to the different location of the metallodrug within the inner pore structure and the exposed pore surface of the nanoparticles, leading to different interactions between the adsorbate and the porous matrix.

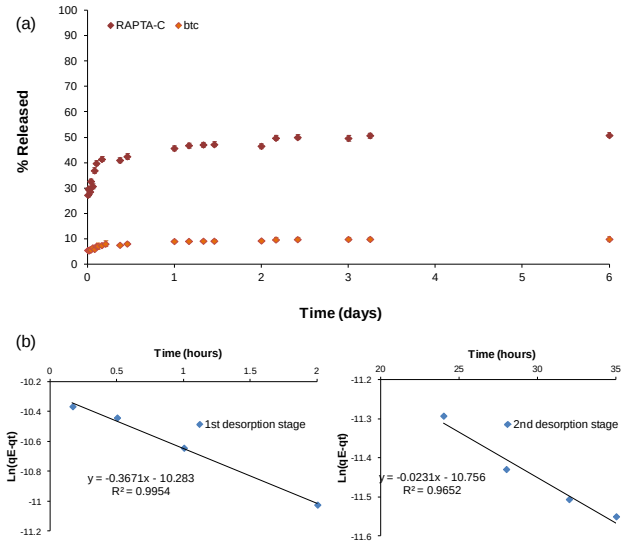

Figure 3. (a) Desorption kinetics profile of RAPTA-C (brown diamonds) and btc release (orange diamonds) from MIL-100(Fe)@RAPTA-C in SBF at 37 °C measured by UV-vis. (b) Fitting of the RAPTA-C desorption data to a first order kinetic model for the 1st (left) and 2nd (right) desorption stages.

Thus, the RAPTA-C molecules might interact by means of π-π stacking between the aromatic ring of the cymene group (RAPTA-C) and the benzene ring of btc linkers present in the MIL-100(Fe) pore structure. However, the external surface of the nanoparticles will probably be formed by defective cavities which will give rise to lower confinement effects of the hosted RAPTA-C molecules. Therefore, the RAPTA-C initial delivery could be related to weakly adsorbed molecules on the external nanoparticles surface (first step), while the RAPTA-C molecules located on the surface of the pore walls, which are strongly retained, will be released in a more slowly way (second step). These results are in agreement with previously reported work on ibuprofen delivery from the porous matrix MIL-100(Fe)@ibuprofen.[23]

Moreover, the two steps of RAPTA-C desorption data can be fitted to a first order kinetic model according to eqn (1):

$$q_E - q_t = q_E e^{-kt} \quad (1)$$

where q_E and q_t are the amounts of RAPTA-C released *per* gram of MOF (mmol g^{-1}) at the equilibrium and at the time t (h), respectively, and k is the first order kinetic constant (h^{-1}). The fitting of the first and second desorption stage obtained by UV-vis gives rise to k values of 0.37 and 0.02 h^{-1} which correspond to half life times (time required for the delivery of the half amount of the drug, $t_{1/2}$) for the release of the metallodrug of 1.9 and 30 hours, respectively. Noteworthy, ca. 50% of the loaded metallodrug is released after 3 days. These results were also confirmed by HPLC (Figure S6). We also followed the eventual degradation of MIL-100(Fe) during the metallodrug release by checking btc leaching. The results showed a related profile to the 1st step of the metallodrug release, with about 10 % of btc leaching after 2 days, which might be indicative that the passive RAPTA-C desorption from the pore structure is coupled to the partial degradation of MIL-100(Fe) nanoparticles which lead to an augmented metallodrug release. Finally, the ICP-OES analysis of the MIL-100(Fe)@RAPTA-C material after being suspended in SBF for 7 days confirmed the presence of Ru, corresponding with a 35% of remaining RAPTA-C into the MIL-100(Fe) matrix. This result is in agreement with the results obtained for the delivery of RAPTA-C by UV-vis and HPLC.

In view of the MIL-100(Fe) nanoparticle degradation in SBF, we studied the eventual effect of the presence of albumin (BSA) on the colloidal stability of MIL-100(Fe).[19]

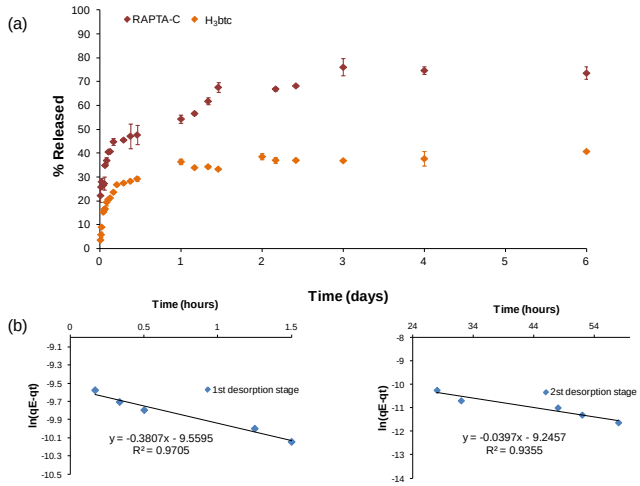

Figure 4. (a) Desorption kinetics profile of RAPTA-C (brown diamonds) and btc release (orange diamonds) from MIL-100(Fe)@RAPTA-C in SBF doped with 5.4% of BSA at 37 °C measured by RP-HPLC. (b) Fitting of the RAPTA-C desorption data to a first order kinetic model for the 1st (left) and 2nd (right) desorption stages.

In order to study the metallodrug releasing process in SBF supplemented with BSA, and since RAPTA-C and BSA UV-vis absorption bands overlap, RP-HPLC was used to follow this process. The HPLC results showed that the first step of the RAPTA-C delivery profile, in SBF@BSA at 37 °C, is similar to the

one performed in SBF, while the second step is more pronounced (Figure 4).

The fitting of the first and second desorption stage gives rise to a *k* value of 0.38 and 0.04 h^{-1} which correspond to a half-life time ($t_{1/2}$) for the release of the metallodrug of 1.8 and 18 hours, respectively. Noteworthy, a higher amount of loaded RAPTA-C is released, after 3 days, namely 80%. This result might be related to the presence of BSA in SBF. In this regard, two effects may operate. On the one hand, it should be pointed out that the amount of leached btc linker in SBF@BSA (~ 40% along the studied period) is more pronounced than in SBF (see above) which should be indicative of a higher degree of degradation of the MIL-100(Fe)@RAPTA-C nanoparticles in this media. Consequently, the RAPTA-C delivery process in SBF supplemented with BSA seems to be coupled to nanoparticle degradation. On the other hand, the presence of albumin may also influence on speeding up the diffusion process of RAPTA-C since albumin protein has been proven to bind and transport a variety of compounds, like fatty acids, bilirubin, metal ions, steroid hormones, vitamins, pharmaceuticals, including metallodrugs.[24] In addition, Dyson and co. demonstrated that the formation of the conjugate albumin@RAPTA-C improves the RAPTA-C's cell growth inhibition in A2780 ovarian carcinoma.[25] Moreover, albumin performs a number of physiologically important functions including the distribution of various compounds, like Ru-metallodrugs. For example, the ruthenium-arene complexes can bind histidine (His128, His247, His510) and methionine (Met298) residues on the surface of albumin, and the *p*-cymene complexes can gain entry to the crevice to bind to the free cysteine thiolate (Cys34, located inside the crevice) and induce oxidation to sulfinate.[26] Moreover, in the presence of albumin the UV-vis absorption band of some Ru-compounds remains stable (i.e. KP1019).[27] All these previously reported results, may explain the higher release of RAPTA-C in the presence of albumin.

Conclusions

In this study, we prove the adsorption of the novel metallodrug RAPTA-C into the pores of MIL-100(Fe), obtaining the loaded matrix MIL-100(Fe)@RAPTA-C. The MIL-100(Fe)@RAPTA-C species embodies the advantages of the use of MIL-100(Fe) as drug delivery system (biocompatible, biodegradable and homogeneous nanoparticles with an optimal colloidal stability), with the antimetastasic activity of the RAPTA-C metallodrug. These features make it an interesting model for the use of MOFs for drug delivery purposes via intravenous administration, as demonstrated by the loading of a significant quantity of RAPTA-C, namely 0.42 g of drug *per* gram of MOF. Moreover, the long half-life of the second step of RAPTA-C delivery in both, SBF and SBF@BSA, offer the possibility to achieve an adequate controlled release of the drug. These results are encouraging and future work on cytotoxicity of the MIL-100(Fe)@RAPTA-C systems are planned to be carried out.

Acknowledgements

This work was supported by MINECO (CTQ2014-53486-R), the Junta de Andalucía (project: P09-FQM-70 4981 and S. R. pre-doctoral and postdoctoral fellowship) and COST Action CM1105.

Notes and references

1 M. Malvezzi, P. Bertuccio, T. Rosso, M. Rota, F. Levi, C. La Vecchia, E. Negri, *Ann. Oncol.*, 2015, **26**, 779-786.
2 P. J. Dyson, G. Sava, *Dalton Trans.*, 2006, 1929-1933.
3 M. Pongratz, P. Schluga, M. A. Jakupec, V. B. Arion, C. G. Hartinger, G. Allmaier, B. K. Keppler, *J. Anal. At. Spectrom.,* 2004, **19**, 46-51; M. A. Jakupec, M. Galanski, V. B. Arion, C. G. Hartinger, B. K. Keppler, *Dalton Trans.,* 2008, 183-194; C. S. Allardyce, P. J. Dyson*, Platinum Metals Rev.*, 2001, **45**, 62-69.
4 A. Casini, F. Edafe, M. Erlandsson, L. Gonsalvi, A. Ciancetta, N. Re, A. Ienco, L. Messori, M. Peruzzini, P. J. Dyson, *Dalton Trans.*, 2010, **39**, 5556-5563; H. Amouri, J. Moussa, A. K. Renfrew, P. J. Dyson, M. N. Ranger, L. –M. Chamoreau, *Angew. Chem. Int. Ed.*, 2010, **122**, 7692-7695.
5 S. Kapitza, M. Pongratz, m. A. Jakupec, P. Heffeter, W. Berger, L. Lackinger, B. K. Keppler, B. Marian, *J. Cancer Res. Clin. Oncol.,* 2005, 101-110.
6 G. Sava, S. Pacor, A. Bergamo, M. Cocchietto, G. Mestroni, E. Alessio, *Chemico-Biological Interactions*, 1995, **95**, 109-126.
7 C. S. Allardyce, P. J. Dyson, D. J. Ellis, S. L. Heath, *Chem. Commum.*, 2001, 1396-1397.
8 Z. Adhireksan, G. E. Davey, P. Campomanes, M. Groessi, C. M. Clavel, H. Yu, A. A. Nazarov, C. H. F. Yeo, W. H. Ang, P. Dröge, U. Rothlisberger, P. J. Dyson, C. A. Davey, *Nat. Commun.*, 2014, **5**, 3462, doi: 10.1038/ncomms4462.
9 W. H. Ang, P. J. Dyson, *Eur. J. Inorg. Chem.*, 2006, 4003-4018.
10 A. Weiss, R. H. Berndsen, M. Dubois, C. Müller, R. Schibli, A. W. Griffioen, P. J. Dyson, P. Nowak-Sliwinska, *Chem. Sci.*, 2014, **5**, 4742.
11 P. Nowak-Sliwinska, J. R. van Beignum, A. Casini, A. A. Nazarov, G. Wagnières, H. van den Bergh, P. J. Dyson, A. W. Griffioen, *J. Med. Chem.*, 2011, **54**, 3895-3902; A. Weiss, X. Ding, J. R. van Beijnum, I. Wong, T. H. Wong, T. H. Wong, R. H. Berndsen, O. Dormond, M. Dallinga, L. Shen, R. O. Schlingemann, R. Pili, C. –M. Ho, P. J. Dyson, H. van der Bergh, A. W. Griffioen, P. Nowak-Sliwinska, *Angiogenesis*, 2015, **18**, 233-244.
12 P. Dyson, International patent WO/2002/040494 A1.
13 C. Scolaro, A. Bergamo, L. Brescacin, R. Delfino, M. Cocchietto, G. Laurenczy, T. J. Geldbach, G. Sava, P. J. Dyson, *J. Med. Chem.,* 2005, **48**, 4161-4171; C. Scolaro, C. G. Hartinger, C. S. Allardyce, B. K. Keppler, P. J. Dyson, *J. Inorg. Biochem.*, 2008, 1743-1748.
14 E. Quartapelle Procopio, S. Rojas, N. M. Padial, S. Galli, N. Masciocchi, F. Linares, D. Miguel, J. E. Oltra, J. A. R. Navarro, E. Barea, *Chem. Commun.,* 2011, **47**, 11751–11753.
15 G. Férey, C. Serre, T. Devic, G. Maurin, H. Jobic, P. L. Llewellyn, G. D. Weireld, A. Vimont, M. Daturi, J. –S. Chang, *Chem. Soc. Rev.,* 2011, **40**, 550-562.
16 S. Rojas, E. Quartapelle-Procopio, F. J. Carmona, M. A. Romero, J. A. R. Navarro, E. Barea, *J. Mater. Chem. B*, 2014, **2**, 2473-2477.
17 A. C. McKinlay, R. E. Morris, P. Horcajada, G. Férey, R. Gref, P. Couvreur, C. Serre, *Angew. Chem. Int. Ed.,* 2010, **49**, 6260-6266; P. Horcajada, T. Chalati, C. Serre, B. Gillet, C. Sebrie, T. Baati, J. F. Eubank, D. Heurtaux, P. Clayette, C. Kreuz, J. Chang, Y. K. Hwang, V. Marsaud, P. Bories, L. Cynober, S. Gil, G. Ferey, P. Couvreur, R. Gref, *Nature Materials*, 2010, **9**, 172-178; M.

Giménez-Marqués, T. Hidalgo, C. Serre, P. Horcajada, *Coord. Chem. Rev.* 2015, in the press.
18 P. Horcajada, R. Gref, T. Baati, P. K. Allan, G. Maurin, P. Couvreur, G. Férey, R. E. Morris, C. Serre, *Chem Rev*., 2012, **112**, 1232-1268.
19 E. Bellido, M. Guillevic, T. Hidalgo, M. H. Santander-Ortega, C. Serre, P. Horcajada, *Langmuir*, 2014, **30**, 5911-5920.
20 C. Tamames-Tabar, D. Cunha, E. Imbuluzqueta, F. Ragon, C. Serre, M. J. Blanco-Prieto, P. Horcajada, *J. Mat. Chem. B*, 2014, **2**, 262-271.
21 Y. Seo, J. Yoon, J. Lee, U. Lee, Y. Hwang, C. Jun, P. Horcajada, C. Serre, J. Chang. *Micro. Meso. Mater.*, 2012, **157**, 137–145.
22 The size of RAPTA-C has been estimated as the diameter of the equivalent sphere occupying the same volume occupied by a CCDC-derived model of the metallodrug, as calculated by SMILE (D. Eufri and A. Sironi, J. Mol. Graphics, 1989, 7, 165).
23 P. Horcajada, C. Serre, M. Vallet-Regí, M. Sebban, F. Taulelle, G. Férey, *Angew. Chem. Int. Ed*., 2006, **45**, 5974-5978.
24 A. R. Timerbaev, C. G. Hartinger, S. S. Aleksenko, B. K. Keppler, Chem. Rev., 2006, **106**, 2224-2248; M. Groessi, M. Terenghi, A. Casini, L. Elviri, R. Lobinski, P. J. Dyson, J. Anal. At. Spectrom., 2010, **25**, 305-313.
25 W. H. Ang, E. Daldini, L. Juillerat-Jeanneret, P. J. Dyson, *Inorg. Chem.*, 2007, **46**, 9048-9050.
26 W. Hu, Q. Luo, X. Ma, K. Wu, J. Liu, Y. Chen, S. Xiong, J. Wang, P. J. Sadler, F. Wang, *Chem. Eur. J.*, 2009, **15**, 6586-6594.
27 B. P. Espósito, R. Najjar, *Coord. Chem. Rev.*, 2002, **232**, 137-149.

Table of content entry

The properties of MIL-100(Fe) nanoparticles as vehicles of a non-conventional half-sandwich ruthenium(II) metallodrug in simulated intravenous conditions has been investigated.